

AD-A260 779 ¹⁰ (2)



REPORT DOCUMENT

1a REPORT SECURITY CLASSIFICATION UNCLASSIFIED		3 DISTRIBUTION/AVAILABILITY OF REPORT Approved for public release; distribution is unlimited	
2a SECURITY CLASSIFICATION AUTHORITY		5 MONITORING ORGANIZATION REPORT NUMBER(S) AFOSR-TR-89-0450	
2b DECLASSIFICATION/DOWNGRADING SCHEDULE		7a NAME OF MONITORING ORGANIZATION Air Force Office of Scientific Research /NL	
4 PERFORMING ORGANIZATION REPORT NUMBER(S)		7b ADDRESS (City, State, and ZIP Code) AFOSR/NL Building 410 Bolling AFB, DC 20332-6448	
6a NAME OF PERFORMING ORGANIZATION New Mexico Institute of Mining and Technology	6b OFFICE SYMBOL (if applicable)	9 PROCUREMENT INSTRUMENT IDENTIFICATION NUMBER AFOSR-89-0450	
6c ADDRESS (City, State, and ZIP Code) Geophysical Research Center / R.E.D. Campus Station Socorro, NM 87801		10 SOURCE OF FUNDING NUMBERS	
8a NAME OF FUNDING/SPONSORING ORGANIZATION AFOSR/NL	8b OFFICE SYMBOL (if applicable) NL	PROGRAM ELEMENT NO. 61102F	PROJECT NO. 2310
8c ADDRESS (City, State, and ZIP Code) Building 410 Bolling AFB, DC 20332-6448		TASK NO. -2310/A1	WORK UNIT ACCESSION NO.
11 TITLE (Include Security Classification) SECOND YEAR INTERIM REPORT FOR AFOSR-89-0450, "REMOTE SENSING OF PRECIPITATION AND ELECTRIFICATION WITH A DUAL-POLARIZATION, COHERENT, WIDEBAND RADAR"			
12 PERSONAL AUTHOR(S) Paul R. Krehbiel and Grant Gray			
13a TYPE OF REPORT Interim / Annual	13b TIME COVERED FROM 7/15/90 TO 7/14/91	14 DATE OF REPORT (Year, Month, Day) 1992 September 15	15 PAGE COUNT 8

16 SUPPLEMENTARY NOTATION

17 COSATI CODES		
FIELD	GROUP	SUB-GROUP

18 SUBJECT TERMS (Continue on reverse if necessary)

93-01470



19 ABSTRACT (Continue on reverse if necessary and identify by block number)

The radar has been upgraded through improvements to the receiver and addition of an inexpensive PC-based Digital Signal Processing system to allow real-time processing and display of radar parameters. A Sun Microsystems SPARCstation was added to the system for processed data archive as well as post analysis. The radar system was shipped to Kennedy Space Center for electrification studies during the summer of 1991.

DTIC
SELECTED
S B D
JAN 27 1993

20 DISTRIBUTION/AVAILABILITY OF ABSTRACT <input checked="" type="checkbox"/> UNCLASSIFIED/UNLIMITED <input type="checkbox"/> SAME AS RPT <input type="checkbox"/> DTIC USERS		21 ABSTRACT SECURITY CLASSIFICATION UNCLASSIFIED	
22a NAME OF RESPONSIBLE INDIVIDUAL		22b TELEPHONE (Include Area Code)	22c OFFICE SYMBOL NL

Second Year Interim Report for AFOSR Grant AFOSR-89-0450
"Remote Sensing of Precipitation and Electrification with a
Dual-Polarization, Coherent, Wideband Radar System"
July 15, 1990 to July 15, 1991

The first year's research provided solid evidence of the capability of dual-polarization radar to detect extensive regions of particle alignment in electrified clouds. As was anticipated in the proposal, we were able to verify that lightning echoes are detectable by 3 cm. radar by observing the cross-polar return. (See "First Year Interim Report for AFOSR Grant AFOSR-89-0450")

During the second year of the contract extensive upgrades to the receiver chain for the radar were made. Real-time signal processing and display systems were added to the system to 1) supplement the existing time-series recording system, and 2) to give the radar operator(s) timely operational information so as to better manage radar resources during an experiment. Completion of the modifications was targeted for June, 1991, so that the system could participate in the Convective and Precipitation Experiment (CaPE) at Kennedy Space Center, Florida, during July/August of 1991.

Modification to the radar receiver were focussed primarily on the intermediate frequency (IF) section where critical analog pre-processing is performed. An IF switching network was installed so that the co- and cross-polar channels are each processed through their own IF chain rather than alternating with the transmitted polarization. This modification significantly improved measurement accuracy and allows a higher gain setting for the weaker cross-polar returns. Filters were placed at critical points in the IF chain to improve rejection of unwanted signals. A modern set of analog drivers was installed to allow electronic selection of the data sources for the A/D converters.

A real-time Digital Signal Processor (DSP) system was added to the existing analog-to-digital (A/D) converter/digital instrumentation recorder scheme in such a way that the data source for the signal processor could be switched transparently between the direct A/D output and previously recorded A/D data from the recorder. A serial housekeeping data stream with antenna angles, time, and other pertinent data was recorded as well. The signal processor cards themselves are off-the-shelf units from Ariel Corp. and employ the Motorola DSP56000 DSP chip. Each card is capable of a peak computational rate of 27 million multiply/accumulate (MAC) operations per second. The system currently requires two such DSP cards.

The DSP cards plug directly into a PC/AT-style computer. A 20 MHz 386 computer was chosen as the host, as it was the fastest available PC style machine at the time of ordering. The host was equipped with 8 megabytes of 0 wait-state memory, an Ethernet card for communication with other systems (SUN IPC's, in particular), and a Super-VGA video card capable of producing 800 x 600 point display resolution in 256 colors. A 500 Megabyte fast hard disk subsystem was added for preliminary data recording. During non-operational times data from the PC/AT disk are transmitted over Ethernet to the SUN IPC's 1 gigabyte disk and then archived onto Digital Audio Tapes (DATs).

DSP software was written to compute, in real-time, mean signal power (P_{hh}), differential reflectivity (Z_{dr}), linear (or circular) depolarization ratio (LDR), Doppler velocity (\bar{V}), cross-polar correlation amplitude (ρ_x), and phase (ϕ_x).

The radar system was shipped via rail to KSC on July 15, 1991, for the CaPE effort.

Radar Scientist/Engineer: Mr. Grant Gray, a radar signal processing specialist formerly at the National Center for Atmospheric Research in Boulder, Colorado, was hired as a full-time project engineer starting 1 July, 1991.

Graduate Students: Support for one graduate student, Tiehan Chen, was provided by the grant during the period. Mr. Chen brought his real-time DSP code to operational status and wrote a data acquisition and display program for the host computer. His work and support will continue through the third year of the grant.

Publications/Reports: The following conference presentations and papers have resulted from the second year's work on this grant:

Rison, W., P. Krehbiel, T. Chen, and P. Gondalia, Design of a PC-based Real-Time Radar Display, *Preprints: 25th International Conference on Radar Meteorology*, AMS. Paris, June 1991. pp 227-228.

Krehbiel, P., W. Rison, S. McCrary, T. Blackman, Dual Polarization Observations of Lighting Echoes and Precipitation Alignment at 3 cm Wavelength, *Preprints: 25th International Conference on Radar Meteorology*, AMS. Paris, June 1991. pp 901-904.

Copies of the above papers and abstracts are attached.

DTIC TAB 3

Accession For	
NTIS GRA&I	<input checked="" type="checkbox"/>
DTIC TAB	<input type="checkbox"/>
Unannounced	<input type="checkbox"/>
Justification _____	
By _____	
Distribution/ _____	
Availability Codes	
Dist	Avail and/or Special
A-1	

DESIGN OF A PC-BASED REAL-TIME RADAR DISPLAY

William Rison, Paul R. Krehbiel, Tiehan Chen, and Paresh Gondalia

Geophysical Research Center
New Mexico Institute of Mining and Technology,
Socorro, New Mexico 87801

Because of the computational power needed to process radar data in real time, radar displays are usually quite expensive. Display processors are often hardwired or micro-coded, making it difficult to adapt them to different modes of display. The New Mexico Tech Wideband, Coherent Radar is a multiparameter radar, for which we want to display mean Doppler velocity, mean reflectivity, differential reflectivity, and linear depolarization ratio. To do this, we built a display which is inexpensive, and is easy to reprogram for different display modes.

The current generation of digital signal processing (DSP) chips provides the computational power to process the radar data in real time. These chips are supported by the manufacturers with extensive software tools, such as assemblers, simulators, compilers and debuggers. Inexpensive plug-in boards with a DSP chip, I/O interfaces, and memory are commercially available. Workstations and personal computers are dropping in price and gaining in performance and display resolution, making them viable alternatives for use as dedicated displays.

The computational heart of our display is a 27 MHz Motorola 56001 DSP chip. This chip executes at 13.5 MIPS, and each instruction can carry out up to five functions—an arithmetic operation on data (such as a multiply-and-accumulate), two parallel data moves, and two address calculations. It operates on a 24-bit wide data word. It has a 24-bit parallel interface for data I/O, built-in hardware for serial I/O, and an 8-bit host port to communicate with a host computer. One nice feature of the 56001 is its zero-overhead interrupt mode. After receiving an interrupt, the 56001 can execute two instructions (such as moving data from memory to the host port) without having to save registers and branch to an interrupt service routine.

We purchased a commercial DSP board with a 56001 chip and 64 k words of zero-wait-state static RAM memory. This board plugs into the bus of a host computer (in our case, an IBM PC/AT 386 clone). All software development is performed on the host, and the assembled programs are uploaded through the host port to the 56001.

A block diagram for the display system is shown in Figure 1. It consists of four major parts—the radar data stream, the hardware interface between the radar and the DSP, the DSP itself, and the host computer with its display monitor.

• **Radar** The radar is a multi-parameter radar which can transmit both horizontally- and vertically-polarized pulses, and receives both polarizations. It can transmit either single frequency for Doppler measurements, or a broadband noise pulse for fast-scanning reflectivity measurements. The received return is digitized at a 1-MHz rate, giving a range resolution of 150 m. For each range gate, the radar produces 6 bytes of data—reflectivity, and I and Q for both vertical and horizontal polarizations. The 6 bytes of data for each range gate are formatted as two 24-bit words—the three bytes of the horizontal return, followed by the three bytes of the vertical return—which are clocked out at a 2-MHz rate.

The sequence of transmitted pulses is selectable. A typical transmission sequence for Doppler studies is to transmit single-frequency pulses with a 4-kHz PRF, and to alternate transmitted polarization from pulse to pulse.

The azimuth, elevation, transmitted polarization, attenuation settings, time, and other auxiliary data are clocked out serially with the digitized return data. A 24-bit sync word is embedded in the serial data stream to indicate the start of each pulse. At 4 kHz PRF (making 250 range gates), each pulse results in 500 twenty-four bit data words and 500 bits of serial data, clocked out at 2 MHz.

• **Interface** A minimal hardware interface buffers the data to the DSP. The parallel data are clocked into First-In-First-Out (FIFO) buffers, so the DSP can access it asynchronously. The serial housekeeping stream goes directly into DSP. A sync detector circuit monitors the serial data, searching for the sync word. When the sync detector recognizes the sync word, it asserts a frame detect output, which the DSP uses to break the serial data stream into individual data words. While the FIFOs are being filled with data from the current pulse, the DSP decodes the serial data to determine how it should process the buffered data.

• **DSP** The Motorola 56001 DSP has built-in hardware to format the serial data stream into 16-bit words. Once formatted, the DSP can determine the polarization and type (noise or single frequency) of the transmitted pulse, from which the DSP determines how to handle the parallel data buffered in the FIFOs. For example, to display differential reflectivity, the DSP executes the following algorithm. It waits until the FIFOs are filled with data from a horizontally-polarized pulse. It reads the data from the FIFOs, discarding all data except $\log Z_{hh}$, the horizontally-polarized reflectivity, which it stores. For the next (vertically polarized) pulse, it reads the parallel data, discarding all but $\log Z_{vv}$, the vertically-polarized reflectivity. It then calculates $\log Z_{hh} - \log Z_{vv}$, and accumulates the difference in an array. After accumulating for a set number of pulses (typically 64), the DSP averages the accumulated values, and is ready to send them to the host computer. The 8-bit data words map directly into one of 256 colors to be displayed on the monitor. The DSP can compute mean reflectivity, Z_{DR} and L_{DR} simultaneously. Thus, for each set of pulses, 750 bytes of information are calculated.

The host computer needs to determine from the azimuth and elevation data where to map the range gate on the display monitor. To ease the computational demands on the host computer, the DSP converts the azimuth and elevation into a single number which the host computer can use as an offset into a look-up table to determine the appropriate mapping. After the pulses are accumulated, the DSP signals the host computer that data are available, and initiates the transfer through the DSP's host port. The DSP side of the transfer is done through zero-overhead interrupts, so the DSP can process the next set of pulses while the transfer of the last set takes place.

• **Host Computer** The host computer acts as the system controller, and updates the display. The host uploads the code to the DSP to activate the appropri-

ate display type. After the DSP has processed one set of pulses, and signals the host that data are available, the host reads and displays the data. The first item read is the offset into the look-up table which the DSP computed from the azimuth and elevation. This is followed by 250 bytes of data for each of the three display types.

For our display, we use a Super VGA (SVGA) graphics adapter and monitor, which has a resolution of 800x600 pixels of 256 colors. Because a range gate may be mapped into more than one pixel, the mapping is non-trivial. The host computer uses the offset it read from the DSP to look into a table which specifies into how many pixels the range gate maps. It then uses the same offset as an index into another table, from which it reads a pointer that points to a memory location holding the address of the first pixel to map. It maps the appropriate color for the range gate into that pixel, increments the pointer to get the address of the next pixel to map, and continues for all the pixels required for that particular range gate. It then increments the table offset, and repeats the process for the next range gate. Thus, the host computer does not need to do any calculations itself; it determines display locations by means of very quick look-ups in pre-computed tables. This requires a large amount of RAM to store the tables—the 4 MB in our computer is sufficient.

We use a PC/AT clone for our display, but other computers should work as well. DSP cards are available on VME bus, NU bus, and S bus cards, and computers which use these buses have very good graphics capabilities. We chose a PC/AT clone because of price, the availability of software tools for programming and debugging the DSP, and the ease of interacting with the hardware under the DOS operating system.

The entire display system cost less than \$10,000—about \$4,000 for the host computer and monitor, \$1,000 for the DSP card, \$1,000 for the software, and \$1,000 for parts to build the hardware interface.

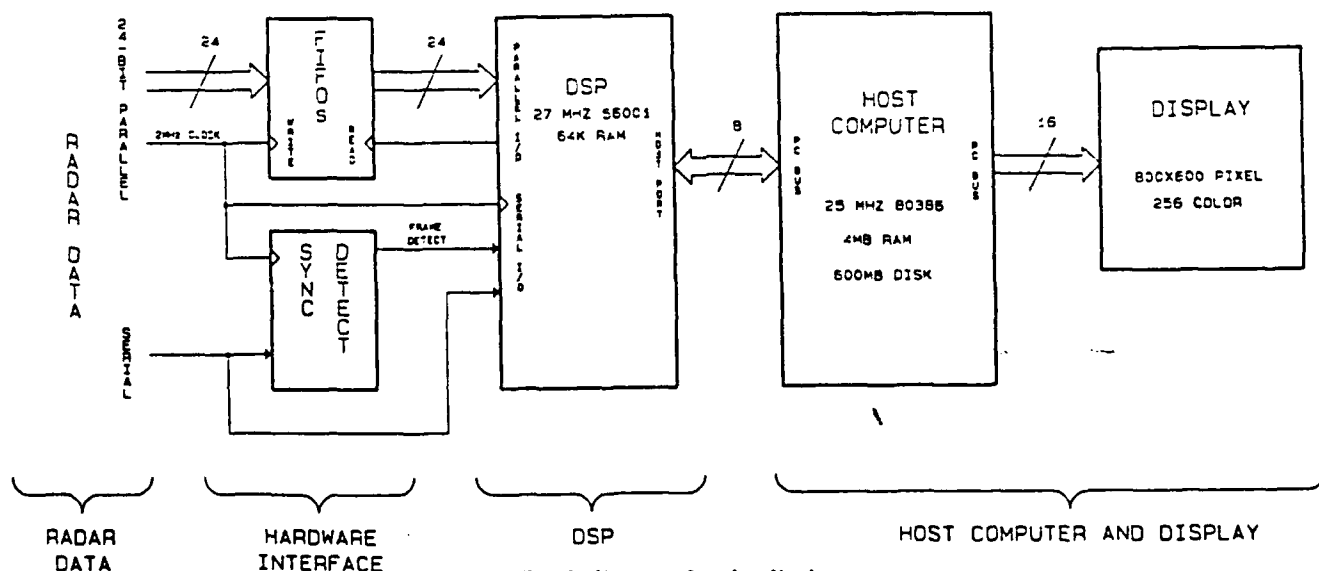


Figure 1. Block diagram for the display system.

DUAL-POLARIZATION RADAR OBSERVATIONS OF LIGHTNING ECHOES AND PRECIPITATION ALIGNMENT AT 3 CM WAVELENGTH.

Paul R. Krehbiel, William Rison, Steve McCrary, Thomas Blackman, and Marx Brook

Langmuir Laboratory, Geophysical Research Center,
New Mexico Tech, Socorro, NM 87801

Polarization-diverse radar observations provide additional information about the precipitation in a storm, but also enable or enhance one's ability to detect and study other storm phenomena. In this paper we describe results in which 3-cm dual-polarization radar measurements have been used to detect manifestations of the electrical activity in a storm - in particular, to detect lightning echoes at short wavelengths and to detect the presence of electrically aligned particles.

Radar echoes from lightning are commonly detected at wavelengths longer than about 5 cm but have rarely been observed at shorter wavelengths ($\lambda \leq 3$ cm). This leads to the question (Williams et al. 1989) whether the lightning channels are underdense at the shorter wavelengths or whether the echoes are simply masked by stronger precipitation echoes. The former would have implications concerning channel electron densities and temperatures while the latter would have implications concerning the electrification processes in a storm.

The detection of electrically aligned particles is of interest because of the possibility for remotely sensing the local electric field or the presence of electrified conditions inside a storm. Electrical alignment has been detected by Hendry and McCormick (1976) from observations of circular polarization returns at 2 cm wavelength, and inferred by Cox and Arnold (1979) from the depolarization of satellite-earth signals. In both instances the particles appeared to be ice crystals and the alignment exhibited sudden changes that were attributed to the occurrence of lightning discharges within the storm.

The measurements of this paper were obtained using linearly-polarized H and V transmissions that alternated from pulse to pulse. The co- and cross-polar returns were received simultaneously in linear (square law) receivers. The attenuation values of the channels were changeable from pulse to pulse to obtain optimum dynamic range. Although the radar is capable also of alternating between coherent single frequency and incoherent noise transmissions, for the measurements of this study the radar transmitted only broadband (300 MHz bandwidth) noise. The noise transmissions enable the clutter fluctuations from precipitation to be substantially reduced (Krehbiel et al. 1979), which improves the ability of the radar to detect transient events.

Figure 1 illustrates the ability of noise transmissions to reduce clutter fluctuations. Shown is the received power vs. range and time in a fixed direction through precipitation. Standard single frequency transmissions produce the noisy clutter returns of Figure 1a; the 300 MHz noise transmissions produce the steadier returns of Figure 1b. For both transmissions the returns are averaged in range for a time equal to the transmitted pulse length (1 μ s).

Figure 2 shows the cross-polar reflected power vs. range and time from a lightning discharge that passed through the (fixed) beam of the radar. The echo lasted about 500 ms and peaked in a single range gate, 22 km from the radar. The narrowness of the echo suggests that it was from a single channel of the discharge. The echo was most prominent in the cross-polar channel due to the decreased attenuation of the receiver for cross-polar returns. Figure 3 shows the simultaneous co- and cross-polar returns and their variation with time. The co-polar return was attenuated by 24 dB relative to the cross-polar return because of precipitation echoes at other ranges. Taking this into account, the cross-polar return was 15-18 dB weaker than the co-polar return.

Figure 4 shows how the lightning echo was correlated with the electrostatic field change of the lightning. (In both this and the earlier figure, the time index is in units of 0.5 ms, corresponding to half the 4 kHz pulse repetition frequency of the radar. The electric field was sampled at the radar prf and was recorded as part of the serial housekeeping data of the radar for good time correlation.) In addition to confirming the lightning nature of the echo, the observations show that the echo began at the same time (within one sample interval) as the electric field change. The long-duration echo at the beginning of the discharge was accompanied by a large initial electric field change, and indicates continuous excitation or current flow along the channel which gradually decreased with time. The impulsive echoes during the final stage of the discharge were associated with step-like electric field changes known as 'k-events'. From optical and photographic observations these are known to produce a transient, high-current discharge along the channel similar to return strokes of cloud-to-ground discharges. The rapid decay of the echo for these events indicates that the channel cools rapidly (in a few ms or less) to an underdense state. The intrinsic cooling rate may be faster than this, as the actual cooling may have been limited by the rate of current decay in the channel.

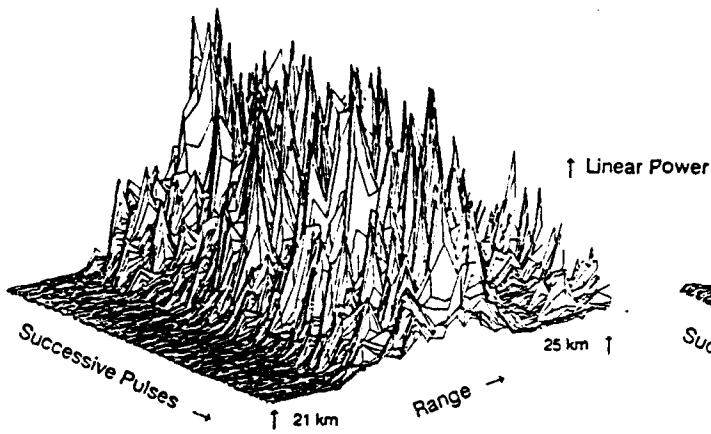


Figure 1a.

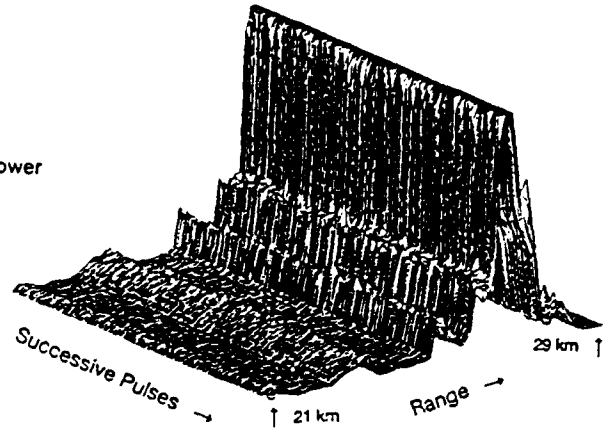


Figure 1b.

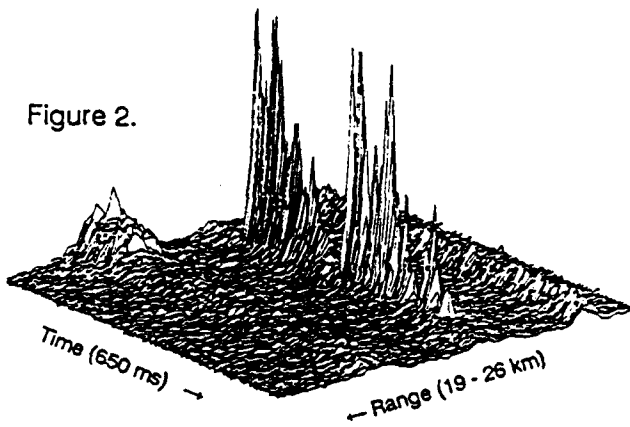


Figure 2.

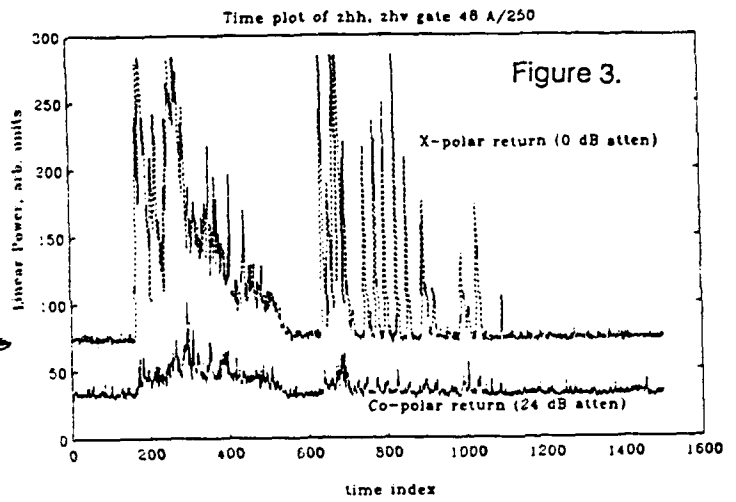


Figure 3.

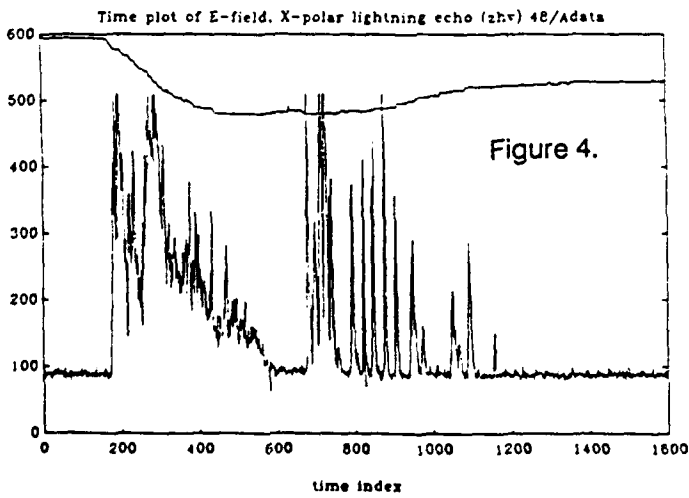


Figure 4.

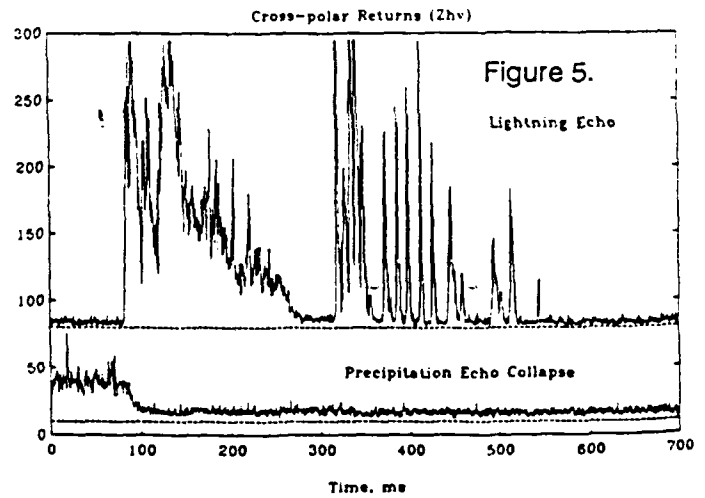


Figure 5.

In addition to the lightning echo, the Figure 2 data also shows the cross-polar return from a precipitation echo, which disappears at the time of the echo. Figure 5 shows the time variation of this return and its correlation with the lightning echo. The precipitation echo collapsed within about 10 ms of the start of the lightning, to below the noise level of the receiver. This indicates that the particles were aligned prior to the discharge, and became de-aligned when the lightning discharge reduced the electric field in the region of the return.

Figure 6 presents 4.5 minutes of observations of the above precipitation echo. During this time, the radar was pointed in a fixed direction 20.5 degrees above the horizon through the upper part of a small, electrically active storm at about 20 km distance. The precipitation echo in question showed up as a localized region of cross-polar return at 24 km slant range on the far side of the storm. The echo was observed in real time on the A-scope of the radar to repeatedly grow and collapse, with the collapses being coincident with the audio output of an optical lightning detector, and often with cross-polar lightning echoes at slightly closer range. This behavior is documented in the figure, which also shows the electric field changes produced by lightning within the storm.

For the first 2 minutes of the Figure 6 data, the cross-polar return exhibited a sawtooth behavior similar to the expected variation of the local electric field in the storm. The cross-polar return would have this time variation if elongated particles were becoming aligned by the local electric field at a non-zero or non-normal angle relative to the polarization vector of the radar. The co-polar return was attenuated by a constant 24 dB relative to the cross-polar return, and changed only slightly and slowly with time. (The small step changes in the co-polar return were caused by single-gate adjustments of the range gate at which the return was sampled.) Detailed comparison with the electric field change record shows that the echo collapses were associated with small negative field changes;

these are known to be due to intracloud lightning in the upper part of the cloud. No cross-polar change (or only a minor change) was associated with the larger positive field changes, which were produced by cloud-to-ground discharges. This is consistent with the fact that CG discharges extend only up to mid-levels in the storm and would be expected to produce a smaller field change in the storm top than IC discharges. (Some field changes were produced by lightning in another storm at a greater distance.)

During the final 2.5 minutes of the record the cross-polar return undulated around a lower value and several lightning events caused the return actually to *increase*. (Two increases also occurred during the first part of the record.) Cross-polar increases can be explained two ways - either the electric field (and therefore the degree of alignment) was stronger after the discharge than before, or the electric field remained strong but changed direction as a result of the lightning. Although the first interpretation is possible, we favor the second interpretation as being consistent with the cross-polar signal between lightning events. In this interpretation, the electric field became approximately aligned with the radar polarization vector (or normal to it), resulting in a minimum cross-polar return which would be sensitive to changes in the alignment direction.

The linear depolarization ratio (LDR) of the aligned particles is somewhat uncertain because of the co-polar attenuation, but appeared to be 3 to 6 dB greater than -24 dB, and varied by a factor of two (3 dB) as the particle alignment changed. Because of their altitude (10.5 km MSL), the particles undoubtedly were ice-form. Other echoes at closer range in the storm had LDR's 6 dB less than -24 dB and did not noticeably change with the occurrence of lightning.

Recent observations (not shown here) at lower altitude above the brightband of a dissipating storm have shown that lightning-associated cross-polar changes occur

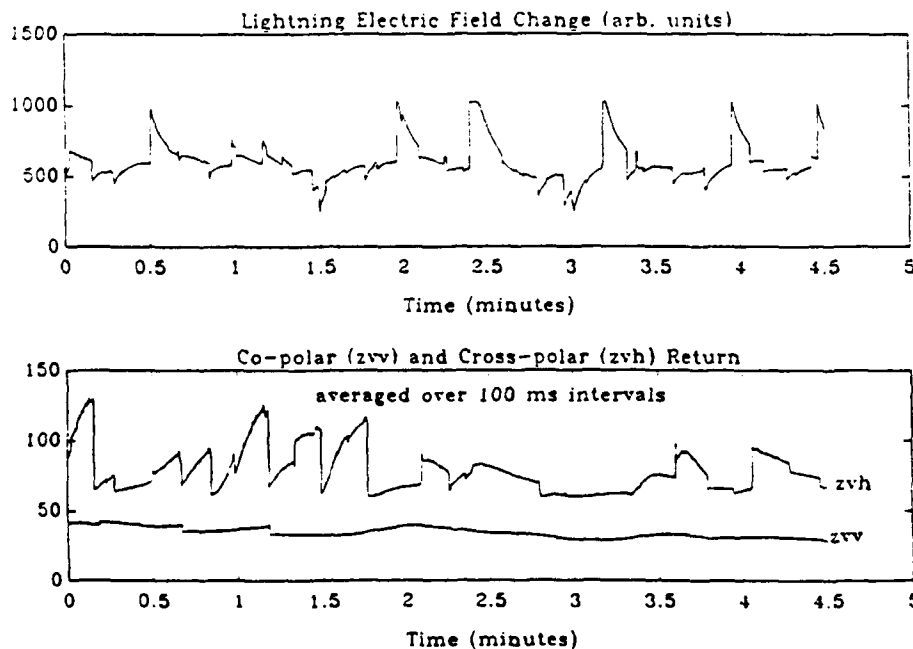


Figure 6.

throughout the horizontal extent of the storm, and indicate that particles commonly become aligned over extensive regions of dissipating storms.

The above observations detect particle alignment using incoherent measurements; of interest in continued studies are coherent measurements, since the co- and cross-polar returns of aligned particles are expected to be correlated. Correlation measurements were used by Hendry and McCormick (1976) to detect alignment and should provide an unambiguous indication of alignment before or in the absence of lightning. Hendry and McCormick also used circular polarization, which they noted would enable the direction of alignment to be ascertained.

In conclusion we return to the lightning echo results. Figure 7 shows volume reflectivity measurements reported by Williams et al. (1989) at longer wavelengths, vs. the observation wavelength. Added to their figure are the apparent (co-polar) volume reflectivities (η) of two representative lightning echoes from the current study. Both co-polar echoes would have been well-masked by 30 dBZ precipitation, or by the normal clutter fluctuations of weaker precipitation. Assuming that the reflectivity values are generally representative of lightning, the lack of observations of lightning echoes at 3 cm wavelength (in comparison with longer wavelengths) implies that the in-cloud portions of discharges tend to be confined to regions of at least mildly

reflecting precipitation. A final comment concerns the wavelength dependence of the lightning reflectivity. The dependence is not well understood; the above results suggest that η is approximately constant between 3 and 10 cm wavelength. Additional observations are needed to test these results.

REFERENCES.

Cox, D.C., and H.W. Arnold, 1979: Observations of rapid changes in the orientation and degree of alignment of ice particles along an earth-space radio propagation path. *J. Geophys. Res.*, 84, 5003-5010.

Hendry, A., and G.C. McCormick, 1976: Radar observations of the alignment of precipitation particles by electrostatic fields in thunderstorms. *J. Geophys. Res.*, 81, 5353-5357.

Krehbiel, P.R., and M. Brook, 1979: A broadband noise technique for fast-scanning radar observations of clouds and clutter targets. *IEEE Trans. Geosci. Elect.*, GE-17, 196-204.

Williams, E.R., S.G. Geotis, and A.B. Bhattacharya, 1989: A radar study of the plasma and geometry of lightning. *J. Atmos. Sci.*, 46, 1173-1185.

Figure 7.

